Acta Crystallographica Section D
Biological Crystallography
ISSN 0907-4449

Crystallization and preliminary structure determination of the C-terminal truncated domain of the S-layer protein SbsC

Tea Pavkov,[a] Monika Oberer,[a] Eva M. Egelseer,[b,c] Margit Sára,[b,c] Uwe B. Sleytr[b] and Walter Keller[a]*

[a]Institute of Chemistry/Structural Biology, Karl-Franzens-University Graz, Heinrichstrasse 28, 8010 Graz, Austria, [b]Center for Ultrastructure Research, Ludwig Boltzmann Institute for Molecular Nanotechnology, University of Agricultural Sciences, Gregor Mendelstrasse 33, 1080 Vienna, Austria, and [c]BMT–Biomolecular Therapeutics GmbH, Brunnerstrasse 59, 1235 Vienna, Austria

Correspondence e-mail: walter.keller@uni-graz.at

Received 28 April 2003
Accepted 16 May 2003

The C-terminal truncated form of the S-layer protein SbsC from *Geobacillus stearothermophilus*, $rSbsC_{31–844}$, has been crystallized by the vapour-diffusion method using polyethylene glycol 6000 as a precipitating agent. The crystals diffract to 3 Å resolution using synchrotron radiation and belong to space group $P2_1$, with unit-cell parameters a = 57.24, b = 98.91, c = 108.62 Å, β = 94.34°. One molecule is present in the asymmetric unit, which corresponds to a solvent content of 65%. Native and heavy-atom derivative data have been collected. The Pt derivative yielded two high-occupancy sites per molecule.

1. Introduction

Crystalline bacterial surface layers (S-layers) can now be considered to be one of the most common surface structures in prokaryotic cells (Sleytr & Beveridge, 1999; Sára & Sleytr, 2000; Sleytr *et al.*, 2000; Sleytr, Sára *et al.*, 2003; Sleytr, Egelseer, 2003). The S-layers of bacteria and archaea are composed of identical protein or glycoprotein subunits and they completely cover the cell surface during all stages of bacterial growth and division. The proteinaceous subunits of S-layers can be aligned in lattices with oblique, square or hexagonal symmetry with a centre-to-centre spacing of the morphological units of approximately 3–35 nm. Depending on the type of S-layer protein, the subunits show a molecular mass of 40–200 kDa. In bacteria, the S-layer subunits are linked to each other and to the underlying cell-envelope layer by noncovalent interactions and can therefore be extracted from the rigid cell-wall layer with high concentrations of hydrogen-bond breaking agents (*e.g.* guanidine hydrochloride). Isolated S-layer subunits have frequently shown an inherent ability to reassemble into two-dimensional arrays in suspension and on interfaces after removal of the disrupting agent used in the dissolution procedure (Sleytr *et al.*, 1988). High-resolution electron-microscopy studies in combination with digital image processing have shown that crystal growth on interfaces is initiated simultaneously at many randomly distributed nucleation points and proceeds in-plane until the crystalline domains meet, thus leading to a closed coherent mosaic of individual several micrometre-large S-layer domains (Pum *et al.*, 1993; Sleytr & Pum, 1996). The formation of these self-assembled arrays is only determined by the amino-acid sequence of the polypeptide chains and consequently the tertiary structure of the S-layer protein species. The shape and size of the self-assembly products strongly depend on the environmental parameters during crystallization such as temperature, pH, ion composition and/or ionic strength (Sleytr *et al.*, 2000). The S-layer subunits may also recrystallize into monomolecular protein lattices on solid supports (*e.g.* gold chips, silicon wafers or plastics), at the air/water interface, on lipid films or liposomes.

Today, potential applications reach from the development of ultrafiltration membranes to biosensors, diagnostic kits, vaccine applications, affinity matrices and many other aspects of molecular nanobiotechnology and biomimetics (Sleytr *et al.*, 1999, 2000, 2002; Pum *et al.*, 2000). Although relatively few data are available on the specific functions of S-layers, there is strong evidence that these crystalline arrays have the potential to function as (i) a cell-shape-determining framework, (ii) protective coats, molecular sieves and molecule or ion traps, (iii) adhesion sites for exoenzymes and (iv) promoters of cell adhesion and surface recognition (Sleytr *et al.*, 1997; Sleytr & Beveridge, 1999; Sleytr, Sára *et al.*, 2003)

The cell surface of *Geobacillus stearothermophilus* ATCC 12980 is completely covered with an oblique lattice (Egelseer *et al.*, 1996) consisting of the S-layer protein SbsC. The *sbsC* gene encoding this S-layer protein has been cloned and sequenced (Jarosch *et al.*, 2000). The protein precursor consists of 1099 amino acids, with a theoretical molecular mass of 115 409 Da and an isoelectric point of 5.73, and includes a typical Gram-positive signal peptide of 30 amino acids. Studies of the biological function revealed that the oblique S-layer lattice from *G. stearothermophilus* ATCC 12980 serves as an adhesion site for a

high-molecular-mass exoamylase (Egelseer *et al.*, 1996). To elucidate the structure–function relationship of distinct segments of SbsC, three N- and seven C-terminal truncations were expressed in *Escherichia coli* HMS174(DE3) (Jarosch *et al.*, 2001). After isolation from the host cells, the self-assembly and recrystallization properties of the truncated rSbsC forms were investigated. It was shown that the N-terminal positively charged segment (amino acids 31–257) interacts with a distinct type of secondary cell-wall polymer by a highly specific lectin-type recognition mechanism, without being involved in the self-assembly process nor being required for the oblique lattice structure (Egelseer *et al.*, 1998; Jarosch *et al.*, 2001; Sára, 2001). This N-terminal part is mainly organized in α-helices connected by loops, as derived from secondary-structure prediction, and seems to fold independently of the remainder of the protein sequence. Three C-terminal truncated forms $rSbsC_{31–713}$, $rSbsC_{31–844}$ and $rSbsC_{31–860}$ had lost the ability to self-assemble and stayed in the water-soluble state whereas the deletion of 199 or even 219 C-terminal amino acids led to self-assembly products exhibiting either a faint or no regular lattice structure. Since high-resolution structural studies on S-layer proteins require three-dimensional crystals, the present study was carried out with the water-soluble form $rSbsC_{31–844}$. Up to now, only a few attempts to crystallize S-layer proteins have been reported (Claus *et al.*, 2002) and only one structure of an archaeal S-layer, the N-terminal part of an *Methanosarcina mazei* surface-layer protein, has been determined (Jing *et al.*, 2002).

2. Protein preparation

Protein expression and purification were performed essentially as described by Jarosch *et al.* (2001). In short, the soluble fraction after lysis was subjected to a fractionated ammonium sulfate (AS) precipitation, in which the majority of the $rSbsC_{31–844}$ protein was found in the 35–45% AS fraction. The pellet was dissolved in a small volume of distilled water and first dialyzed against distilled water and then against buffer *A* (2 *M* guanidine hydrochloride, 150 m*M* NaCl, 50 m*M* Tris pH 7.2). After centrifugation, the supernatant was applied onto a Superdex 200 column (Pharmacia) and eluted with buffer *A*. $rSbsC_{31–844}$-containing fractions were pooled, dialyzed against distilled water, lyophilized and dissolved in a small volume of buffer *A*. Subsequently, the sample was reapplied onto the Superdex 200 column under the same elution conditions. Protein-containing fractions were again pooled, dialyzed against distilled water and lyophilized.

3. Crystallization

A lyophilized sample of $rSbsC_{31–844}$ was dissolved and dialyzed overnight against distilled water. The protein concentration (5 mg ml^{-1}) was determined from absorbance measurements at 280 nm using the calculated extinction coefficient of 40 960 M^{-1} cm^{-1} (Gill & von Hippel, 1989). Initial crystallization conditions were found using Crystal Screens I and II (Hampton Research) which produced small crystal clusters. Optimization of crystallization conditions included variation of the pH and the concentration of all the components in the crystallization cocktail. Crystals were grown by sitting-drop vapour diffusion at 293 K. The drops contained equal volumes (1.5 µl) of protein and reservoir solution and were equilibrated against 1 ml of reservoir solution. Crystallization at 277 K gave spherical aggregates which were optically active but did not diffract in the X-ray beam. Plate-like crystals, mainly growing in clusters, were obtained at 293 K from reservoirs consisting of 5–8%(*w*/*v*) PEG 6000 (Fluka), 0.05–0.2 *M* NaCl, 0.1 *M* cacodylate pH 5–6.5. They appeared within one week and were up to 0.6 × 0.4 × 0.1 mm in size. The crystals diffracted to 3.5–4 Å on a rotating copper anode and at the synchrotron. Preliminary X-ray studies were performed at room temperature and at 100 K. To improve crystal quality, streak-seeding was applied. Single crystals appeared within 2–5 d (Fig. 1) and diffracted to 3 Å using synchrotron radiation, with a typical diffraction pattern as shown in Fig. 2.

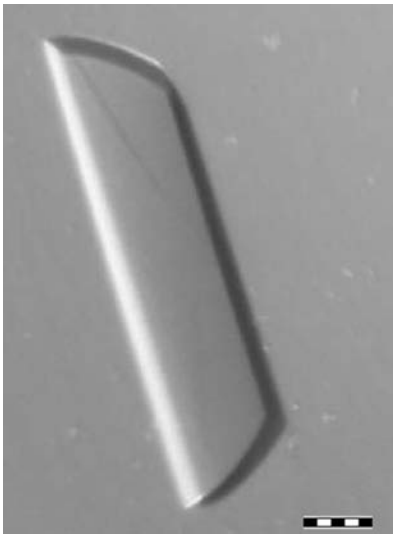

Figure 1
A typical crystal of $rSbsC_{31–844}$ grown in a sitting-drop setup at 293 K in 5%(*w*/*v*) PEG 6K, 0.05 *M* NaCl and 0.1 *M* cacodylate pH 6.0. Scale bar: 50 µm.

4. Data collection and heavy-atom derivative search

Since there are no protein structures available that show a significant sequence homology with $rSbsC_{31–844}$, molecular replacement cannot be used for structure determination. Therefore, various heavy-atom derivatives were prepared and tested for diffraction. The concentration and soaking times were varied in order to maintain the diffraction quality of the crystals. For the data collection, crystals were frozen in liquid nitrogen after gradually adding glycerol (to 20%) to the drop. Native and several potential heavy-atom derivative data sets were collected at the EMBL Outstation at the DORIS storage ring, DESY, Hamburg. All data sets were processed and scaled with the *HKL* programs *DENZO* and *SCALEPACK* (Otwinowski & Minor, 1997). Isomorphous difference and anomalous difference Patterson maps were calculated using the program *FFT* within the *CCP*4 package (Collaborative Computational Project, Number 4, 1994). Data obtained from a crystal soaked in 1 m*M* K_2PtCl_4 for 5 h showed strong peaks in an anomalous difference Patterson map (Fig. 3.). Consistent Pt heavy-atom positions were determined from Patterson maps (position 1: 0.0345, 0, 0.1092; position 2: 0.0242, 0.4365, 0.2444). Data-collection and processing statistics are presented in Table 1.

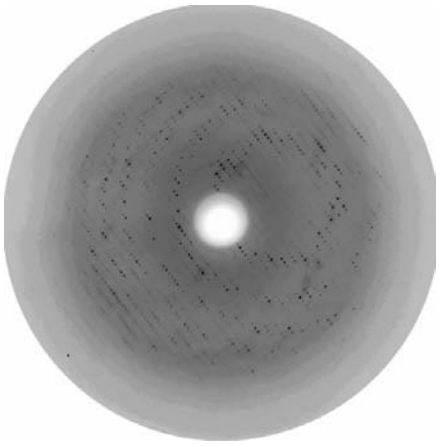

Figure 2
The diffraction pattern of a native $rSbsC_{31–844}$ crystal using synchrotron radiation at beamline X13 (DESY, Hamburg). The outer edge of the plate is at 2.3 Å.

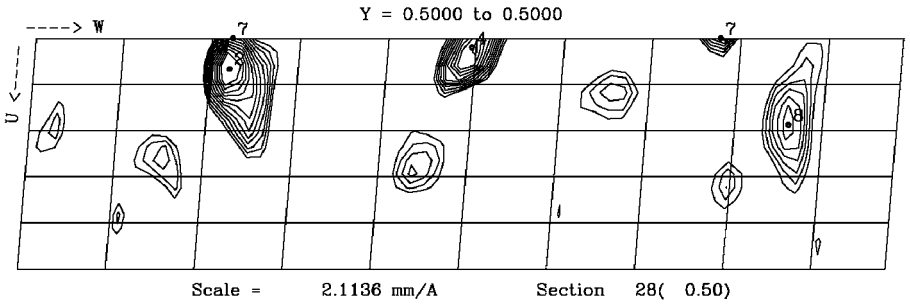

Figure 3
Anomalous difference Patterson map showing the 'Pt' peaks in the $v = 0.5$ Harker section.

Table 1
Data-collection and processing statistics.

Data were collected at 100 K using synchrotron radiation. Values in parentheses refer to the highest resolution shell.

	Native	Pt derivative
Beamline	X13	BW7B
Detector	MAR CCD	MAR CCD
Wavelength (Å)	0.8010	0.8431
Resolution range (Å)	25–3 (3.05–3.0)	25–3.2 (3.26–3.2)
Space group	$P2_1$	$P2_1$
Unit-cell parameters (Å, °)	a = 57.24, b = 98.91, c = 108.62, β = 94.34	a = 57.29, b = 99.32, c = 108.58, β = 94.38
No. observations	74124	62801
No. unique reflections	23384 (1120)	20104 (958)
Completeness (%)	98.5 (94)	99.2 (99.2)
Average $I/\sigma(I)$	12.1 (3.1)	13.38 (3.71)
$R_{sym}(I)$ (%)	7.5 (38.0)	6.4 (28.6)

The calculated Matthews coefficient of 3.52 Å^3 Da^{-1} (Matthews, 1968) indicates that one monomer of rSbsC$_{31–844}$ is present in the asymmetric unit, corresponding to a solvent content of 65%. For a dimer of rSbsC$_{31–844}$, the Matthews coefficient would be 1.7 Å^3 Da^{-1} and the solvent content 28%. In order to exclude this possibility, a self-rotation function was calculated (using *MOLREP* from the *CCP*4 package; Collaborative Computational Project, Number 4, 1994) which did not show any significant peaks, also suggesting that there is only one molecule of rSbsC$_{31–844}$ per asymmetric unit. In addition, size-exclusion chromatography was performed and showed that rSbsC$_{31–844}$ is a monomer in solution (data not shown).

A MAD experiment will be performed with the high-occupancy Pt derivative and the data will be used for structure determination. This structure will provide insight into the molecular architecture of one of the main components of the bacterial cell envelope.

Support during data collection at the DESY by the EMBL staff is gratefully acknowledged. Data collection was supported by a travel grant from the European Community (Access to Research Infrastructure Action of the Improving Human Potential Programme to the EMBL Hamburg Outstation, contract No. HPRI-CT-1999-00017). This work was supported by the Austrian Science Foundation – FWF (grants P12559-GEN and P15040).

References

Claus, H., Akca, E., Debaerdemaeker, T., Evrard, C., Declercq, J. P. & Konig, H. (2002). *Syst. Appl. Microbiol.* **25**, 3–12.
Collaborative Computational Project, Number 4 (1994). *Acta Cryst.* D**50**, 760–763.
Egelseer, E. M., Leitner, K., Jarosch, M., Hotzy, C., Zayni, S., Sleytr, U. B. & Sára, M. (1998). *J. Bacteriol.* **180**, 1488–1495.
Egelseer, E. M., Schocher, I., Sleytr, U. B. & Sára, M. (1996). *J. Bacteriol.* **178**, 5602–5609.
Gill, S. C. & von Hippel, P. H. (1989). *Anal. Biochem.* **182**, 319–326.
Jarosch, M., Egelseer, E. M., Huber, C., Moll, D., Mattanovich, D., Sleytr, U. B. & Sára, M. (2001). *Microbiology*, **147**, 1353–1363.
Jarosch, M., Egelseer, E. M., Mattanovich, D., Sleytr, U. B. & Sára, M. (2000). *Microbiology*, **146**, 273–281.
Jing, H., Takagi, J., Liu, J. H., Lindgren, S., Zhang, R. G., Joachimiak, A., Wang, J. H. & Springer, T. A. (2002). *Structure*, **10**, 1453–1464.
Matthews, B. W. (1968). *J. Mol. Biol.* **33**, 491–497.
Otwinowski, Z. & Minor, W. (1997). *Methods Enzymol.* **276**, 307–326.
Pum, D., Neubauer, A., Györvary, E., Sára, M. & Sleytr, U. B. (2000). *Nanotechnology*, **11**, 100–107.
Pum, D., Weinhandl, M., Hodl, C. & Sleytr, U. B. (1993). *J. Bacteriol.* **175**, 2762–2766.
Sára, M. (2001). *Trends Microbiol.* **9**, 47–49.
Sára, M. & Sleytr, U. B. (2000). *J. Bacteriol.* **182**, 859–868.
Sleytr, U. B. *et al.* (1997). *FEMS Microbiol. Rev.* **20**, 151–175.
Sleytr, U. B. & Beveridge, T. J. (1999). *Trends Microbiol.* **7**, 253–260.
Sleytr, U. B., Egelseer, E. M., Pum, D. & Schuster, B. (2003). *Nanobiotechnology*, edited by C. M. Niemeyer & C. A. Mirkin. Weinheim: Wiley-VCH. In the press.
Sleytr, U. B., Messner, P. & Pum, D. (1988). *Methods Microbiol.* **20**, 29–60.
Sleytr, U. B., Messner, P., Pum, D. & Sára, M. (1999). *Angew. Chem. Int. Ed.* **38**, 1034–1054.
Sleytr, U. B. & Pum, D. (1996). *Crystalline Bacterial Cell Surface Proteins*, edited by U. B. Sleytr, P. Messner, D. Pum & M. Sára, pp. 175–209. Austin, TX, USA: R. G. Landes Co.
Sleytr, U. B., Sára, M. & Pum, D. (2000). *Supramolecular Polymers*, edited by A. Ciferri, pp. 177–213. New York/Basel: Marcel Dekker.
Sleytr, U. B., Sára, M., Pum, D. & Schuster, B. (2002). *Nano-Surface Chemistry*, edited by M. Rosoff, pp. 333–389. New York/Basel: Marcel Dekker.
Sleytr, U. B., Sára, M., Pum, D., Schuster, B., Messner, P. & Schäffer, C. (2003). *Biopolymers*, Vol. 7, edited by A. Steinbüchel & S. Fahnestock, pp. 285–338. Weinheim, Germany: Wiley–VCH.